UNIVERSITÀ DI PARMA
ARCHIVIO DELLA RICERCA

University of Parma Research Repository

Landslide time-of-failure forecast and alert threshold assessment: A generalized criterion

This is the peer reviewd version of the followng article:

*Original*
Landslide time-of-failure forecast and alert threshold assessment: A generalized criterion / Segalini, A., Valletta, A., Carri, A.. - In: ENGINEERING GEOLOGY. - ISSN 0013-7952. - 245:(2018), pp. 72-80. [10.1016/j.enggeo.2018.08.003]

*Availability:*
This version is available at: 11381/2849383 since: 2021-10-13T12:08:47Z

*Publisher:*
Elsevier B.V.

*Published*
DOI:10.1016/j.enggeo.2018.08.003

*Terms of use:*

Anyone can freely access the full text of works made available as "Open Access". Works made available

*Publisher copyright*

note finali coverpage

(Article begins on next page)

07 October 2026

# Landslide time-of-failure forecast and alert threshold assessment: a generalized criterion

**A. Segalini[a], A. Valletta[b], A. Carri[a]**

**[a] Università degli Studi di Parma, DIA, Parco Area delle Scienze 181/A, Parma 43124, Italy**

**[b] Sapienza Università di Roma – CERI, Piazzale Aldo Moro 5, Roma 00185, Italy**

**Corresponding author: A. Segalini – email: andrea.segalini@unipr.it tel: +39 0521905952**

**ORCID: 0000-0001- 8023-9326**

**Abstract**

The forecast of a landslide's time of failure and the definition of alert thresholds are fundamental aspects in the study of natural hazards. However, these tasks are particularly difficult due to the large number of parameters and factors involved, and are therefore usually performed with a site-specific approach. This work describes an attempt to generalize the behavior of a landslide approaching collapse, with particular attention to the definition of a general criterion to define alert thresholds. The procedure started with the creation of a database of displacement data recorded for historical landslides, then the inverse velocity model was applied to these datasets to evaluate the time of failure under the assumption of linear behavior during the accelerating phase. A model calibration was conducted to best describe the monitored data and highlight any non-linear trend. A curve describing the velocity versus time relationship was then computed for each single slope failure case using the parameter obtained through this operation. In the final step of the study, these curves were processed with a normalization procedure, thus obtaining a dimensionless velocity-related coefficient. This parameter allowed the comparison of different landslide datasets on a single graph, which can be used as a general reference to define alert thresholds for emergency purposes. In order to test the criterion's ability to represent landslide behavior, the procedure was also applied to a different case by simulating progressive data acquisition.

**Keywords**

Landslides, creep, failure forecast, monitoring data, alert thresholds, EWS

**Glossary**

$t_f$: time of failure
EWS: Early Warning System
$t$: time
$u$: displacements
InSAR: Interferometric Synthetic Aperture Radar
$v$: velocity
$A$, $\alpha$: Fukuzono empirical parameters
$R^2$: Correlation parameter
GRG: Generalized Reduced Gradient
RMSE: Root Mean Square Error
$v_{FV}$: velocity computed with the Fukuzono-Voight model
$\mu_{vFV}$: mean of the $v_{FV}$ values
$\sigma_{vFV}$: standard deviation of the $v_{FV}$ values
$v_n$: normalized velocity

## 1. Introduction

Within the framework of natural risk management and reduction, the prediction of a landslide occurrence is a particularly relevant task from both a scientific and a socio-cultural point of view. Accurate time-of-failure ($t_f$) forecasting could be a key element to develop an Early Warning System, in order to avoid or at least reduce damage and human losses. However, this is one of the most challenging problems regarding slope stability analysis, due to the large number of factors and parameters influencing landslide behaviour and its triggering, and has been the main focus of several studies.

A first approach was presented in the early 1960s, when Saito and Uezawa (1961) proposed a method based on the comparison between displacement records and creep rupture curves obtained from load-controlled triaxial tests. Saito went on to present successful applications of this method in further studies (Saito, 1969; 1979). Relevant improvements to Saito's theory were achieved, thereby leading to the development of a phenomenological method by Fukuzono (1985) based on small-scale laboratory tests. Results show that the inverse of displacement velocity decreases with time during the tertiary creep phase, characterized by an acceleration of slope deformation. Thus, the time of failure can be forecasted by locating the point where the line interpolating the monitoring data intercepts the x-axis, corresponding to a theoretical infinite velocity. The effectiveness of this method has been proven by various studies concerning retrospective analysis of different cases, such as open pit mines (Carlà et al., 2017a), experimental man-made slopes (Petley, 2004), and catastrophic natural events (Kilburn and Petley, 2003). More recently, Mufundirwa et al. (2010) proposed another method to assess $t_f$ based on a $t(du/dt) – du/dt$ curve, where $u$ and $t$ indicate displacement and time, respectively. Time-of-failure estimation can be obtained by evaluating the slope of this curve.

Following the development of these methods, several authors discussed the possibility of defining alert thresholds levels. Cruden and Masoumzadeh (1987) proposed three velocity levels, corresponding to three accelerating creep stages, with reference to a specific section of an open-pit mine. The main objective was to define a critical time when evacuation of pit personnel and equipment should begin. Intrieri et al. (2012) approached the task by studying the most critical periods

of the entire dataset of the Torgiovannetto landslide, and subsequently derived three different velocity threshold levels to be implemented in an *ad-hoc* EWS. Crosta and Agliardi (2002) applied Voight's model in order to define "characteristic velocity curves" representing the theoretical behaviour of the Ruinon landslide approaching failure. Each curve refers specifically to a monitored sub-area of the landslide, and can be used to define velocity thresholds: for the specific case presented in the paper, the authors chose 30- 15- and 7-day alert velocity thresholds. Manconi and Giordan (2015) adopted a different approach, proposing an EWS where the definition of the alert levels is integrated with a time-of failure-prediction model. By evaluating the model's reliability, a specific threshold can be updated thanks to a near-real time monitoring system.

A generalization procedure is discussed in this paper in order to overcome the site-specific feature associated with these thresholds. Considering that the computational cost of the evaluation of specific alert levels becomes gradually higher as the number of monitored landslide increases, the definition of a generalized criterion could prove useful to set appropriate thresholds according to the case.

# 2. Material and Methods

## 2.1. Time-of-failure forecast methods

As previously stated, a series of different methods have been developed to solve the challenging problem of time-of-failure evaluation. Federico et al. (2012) provided a study where these approaches are investigated from an analytical point of view, also by taking into consideration different monitoring technologies that can be applied to obtain useful parameters. Moretto et al. (2017) also studied this subject by examining different monitoring activities related to historically recorded landslides, and analysed the reliability of four different failure forecast methods (FFMs) based on the available data. Particular attention has been paid to satellite-based technologies, notably InSAR (Interferometric Synthetic-Aperture Radar), while other authors have explored different techniques such as Persistent Scatter Interferometry (Wasowski and Bovenga, 2014) to improve monitoring quality (examples of this approach are presented in Herrera et al., 2013 and Wasowsky et al., 2014).

These methods use different approaches to the time-of-failure evaluation process, but are all based on the assumption that displacements display continuous acceleration, following a hyperbolic trend before failure occurrence. This behaviour is called "accelerating creep", or "tertiary creep", and is described by the creep theory. Terzaghi (1950) first approached the correlation between the accelerating phase and landslide movements, and research carried out by other authors identified the presence of relevant creep deformations before failure (Ter-Stepanian, 1980; Tavenas and Leroeuil, 1981). As for the ability of each specific method to accurately predict the time of failure of a landslide, Intrieri and Gigli (2016) applied the three approaches proposed by Saito (1961), Fukuzono (1985) and Mufundirwa (2010) to different cases, also trying to assess the influence of different factors in the failure forecast process. The effectiveness of each method is represented by a Predictability Index (PI), ranging from 1 to 5, evaluated for each specific landslide monitored. The results showed a similar performance of the Saito and Fukuzono models, while the approach proposed by Mufundirwa generally performed more poorly. The authors noted that the Saito and Fukuzono methods achieved different results in terms of quality with respect to the specific cases, underlining the independence and non-redundancy of these models.

Based on the results reported in literature, which show good effectiveness in time-of-failure forecast, the inverse velocity method is applied in this paper. Due to its easier applicability, it is also more suited to obtain a faster prediction compared to other approaches, which can prove to be a crucial factor in guaranteeing EWS efficiency.

## 2.2. Inverse velocity method

As previously stated, the inverse velocity method developed by Fukuzono (1985) relies on the interpretation of the tertiary creep phase, where the material displacements follow an accelerating trend ultimately leading to the landslide collapse. By studying small-scale models, the author derived proportionality, represented by a power law equation, between the logarithm of acceleration and the logarithm of velocity. Starting from this hypothesis, the author proposed the following equation as an instrument to evaluate landslide time of failure:

$$\frac{1}{v} = \left(A(\alpha - 1)\left(t_f - t\right)\right)^{\frac{1}{\alpha - 1}} \qquad [1]$$

where $v$ represents the surface velocity and $t_f$ is the time of failure. The trend of the inverse-velocity vs time curve depends on parameter $\alpha$, which controls the linearity or non-linearity of the plot. As stated by Fukuzono (1985; 1990), the value of this parameter usually ranges between 1.5 and 2.2 for natural slopes. The hypothesis of linearity, corresponding to $\alpha$=2, is generally a good assumption to estimate the time of failure, especially when data close to failure are considered for the analysis (Rose and Hungr, 2007). It is worth noting that, when slopes influenced by man-made structures are considered, lower values of $\alpha$ are frequently obtained (Bozzano et al. 2014).

From a physical point of view, the Fukuzono model was studied in detail and validated by Voight (1988, 1989), who interpreted the equation as a fundamental law governing various forms of material failure. The result is a general relationship describing the behaviour of materials in terminal stage of failure:

$$\ddot{u} = A\dot{u}^{\alpha} \quad [2]$$

where $\ddot{u}$ and $\dot{u}$ are the displacements acceleration and velocity, respectively. As stated by the author, the term $u$ could be interpreted in terms of conventional geodetic observation, seismic quantities or geochemical observation (Voight 1988). Following this line, the same equation has been successfully implemented to predict volcanic eruptions (Voight 1988; 1990; Cornelius and Voight 1995).

While the inverse velocity method has proven to be an effective and useful resource in different instances, it is necessary to specify that its application must be carefully evaluated depending on the case. In particular, the value of $t_f$ should not be considered as an exact prediction of the landslide collapse, since the method applied generally indicates that the failure is likely in proximity of the intersection point (Carlà et al., 2018). Following this concept, Carlà et al. (2017b) proposed an approach based on long-time and short-time moving average evaluation, aimed to identify the "time window" during which the collapse could take place.

Moreover, when applying this procedure to predict the time of failure of a landslide, these considerations regarding the method's applicability should be taken into account:

- Since the monitoring activity of slope displacements is only one aspect of a very complex phenomenon (i.e. predisposing factors and driving forces), this method should not be applied in isolation.
- Generally, the inverse velocity model struggles to represent brittle failures properly, due to the extremely rapid evolution of a rock mass displaying this behaviour. However, as noted by Carlà et al. (2017b), significant improvements to this problem can be achieved by using a high-frequency monitoring system able to accurately represent the accelerating phase.
- As stated by Intrieri and Gigli (2016), natural or instrumental noise can hinder time-of-failure prediction, therefore data processing operations are recommended to improve the prediction reliability (Mazzanti et al., 2015; Dick et al., 2015).
- The possibility of trend changes, driven by observable or unknown factors, should always be kept in mind. Because of this, it is recommended to continue the monitoring activity as long as possible prior to failure and to constantly update the model with new data to improve the forecast procedure (Rose and Hungr, 2007).

Even with its limitations, the approach proposed by Fukuzono has proven to be a successful tool to track the landslide evolution, allowing its integration in different EWSs for risk reduction purposes (Atzeni et al., 2015; Manconi and Giordan, 2016; Sättele et al., 2016). In this paper, the authors applied the inverse velocity method to analyse historical landslides datasets, in order to forecast the time of failure and, subsequently, derive a series of normalized velocity curves.

### 2.3. Historical landslides collection

The following approach was adopted to achieve the goal of this study:

- creation of a database including historical landslides reported by scientific literature, complete with pre-failure displacement or velocity data recorded by different monitoring systems;
- plotting of a graph with this information through digitizing software;
- application of the Fukuzono model on the dataset in order to forecast the time of failure of the specific landslide;
- calibration of the $A$ and $\alpha$ parameters of the model to obtain a better interpolation of the recorded dataset;
- definition of a characteristic velocity curve for each single case describing the landslide's behaviour during the 30 days before failure occurrence;
- normalization of this curve to assess a generalized series of velocity versus time-to-failure curves.

The cases collected (Table 1) show relevant differences, depending on the typology of the system implemented to monitor the landslide evolution. A variation in the quality and frequency of acquisition was observed. Some of the landslides included in the database were monitored for a time long enough to show the transition between the secondary and tertiary creep phase, while other data series were recorded once the accelerating phase had already started. Other relevant differences are present in terms of volume, materials, failure mechanism and triggering factors.

| Name | Volume [$m^3$] | Material | Failure Mechanism | Trigger | Monitoring duration [d] | References |
|---|---|---|---|---|---|---|
| **Afton Mine** | $28x10^6$ | Rock | Toppling | Excavation, Blasting | 68 | Glastonbury and Fell, 2002 |
| **Asamushi** | $1x10^5$ | Rock | Sliding | Weathering | 7 | Saito, 1969 |
| **Betze Post SE** | $18x10^6$ | Rock | Compound | Groundwater | 45 | Rose and Hungr, 2007 |
| **Betze Post SW** | $2x10^6$ | Rock | Rock Slide | Rainfall | 5 | Rose and Hungr, 2007 |
| **Bomba** | $12x10^6$ | Soil | Slump | Excavation | 1290 | Urciuoli and Picarelli, 2008 |
| **Braced up Cliff** | $1.2x10^4$ | Rock | Toppling | Frost Action, Snow Melt | 1886 | Schumm and Chorley, 1964 |
| **Cavallerizzo** | $5x10^6$ | Rock, Soil | Rock Slide, Earth Flow | Rainfall, Snowfall | 7 | Iovine et al., 2006 |
| **Chuquicamata** | $4.1x10^6$ | Rock | Compound | Excavation, Seismic Actions | 140 | Voight and Kennedy, 1979 |
| **Delabole Quarry** | - | Rock | Toppling | Rainfall | 5900 | Boyd et al., 1973 |
| **Dosan Line** | $6x10^4$ | Rock | Flow | Erosion | 3 | Saito, 1969 |
| **Hogart Pit** | $2x10^5$ | Rock | Toppling | Rainfall, Snow Melt, Excavation | 285 | Brawner and Stacey, 1979 |
| **Huanglongxi** | $3.9x10^5$ | Rock | - | Rainfall, Human Activities | 6 | Li et al., 2012 |
| **La Chenaula** | $1.6x10^6$ | Rock | Roto-Translation | Toe Erosion | 912 | Noverraz and Bonnard, 1992 |
| **La Saxe** | $8.4x10^6$ | Rock | Rock Slide | Snow Melt | 30 | Manconi and Giordan, 2016 |
| **Maoxian** | $18x10^6$ | Rock | Rock Avalanche | Rainfall | 1014 | Intrieri et al., 2018 |
| **Mt Beni** | $5x10^6$ | Rock | Rock Slide, Toppling | Water and Snow | 240 | Gigli et al., 2011 |
| **Nevis Bluff** | $3.2x10^4$ | Rock | Rotation | Excavation | 272 | Brown et al., 1980 |
| **Ohto** | $2x10^5$ | Rock | Rock Slide | Rainfall (Typhoon) | 90 | Suwa et al., 2010 |
| **Ooigawa** | $6x10^4$ | Soil | Earth Flow | Erosion | 10 | Saito, 1969 |
| **Preonzo** | $2.2x10^5$ | Rock | Rockfall | Rainfall | 12 | Geoprævent, 2012 |
| **Puigcercòs** | $10.12x10^5$ | Rock | Rockfall | Gradual Degradation | 2217 | Royàn et al., 2015 |
| **Selborne** | $1.8x10^4$ | Soil | Roto-Translation | Groundwater | 400 | Petley, 2004 |
| **Town of Peace River** | - | Rock | Roto-Translation | Rainfall | 180 | Kim et al., 2010 |
| **Tuckabianna West** | $1.25x10^6$ | Rock | Translation | Excavation | 37 | Glastonbury and Fell, 2002 |
| **Vajont** | $270x10^6$ | Rock | Roto-Translation | Groundwater | 70 | Sornette et al., 2004 |
| **Xintan** | $30x10^6$ | Rock | Rock Slide | Rainfall, Groundwater | 2550 | Keqiang and Sijing, 2006 |

Table 1 - Landslides database collected from scientific literature including details about volume, material, failure mechanism, triggering factors, duration of the monitoring period, and reference

Since the recorded data are displayed in different units depending on the case, all the datasets were converted into mm/d so as to be able to compare different cases. The monitoring data reported in scientific literature were digitized using the software *Engauge Digitizer*, thus allowing the application of the inverse velocity method and the time-of-failure prediction. An example of this operation is presented in Fig. 1, reporting the displacement-time graph relative to benchmark #5 of the Vajont landslide (after Sornette et al., 2003) and the resultant digitized dataset.

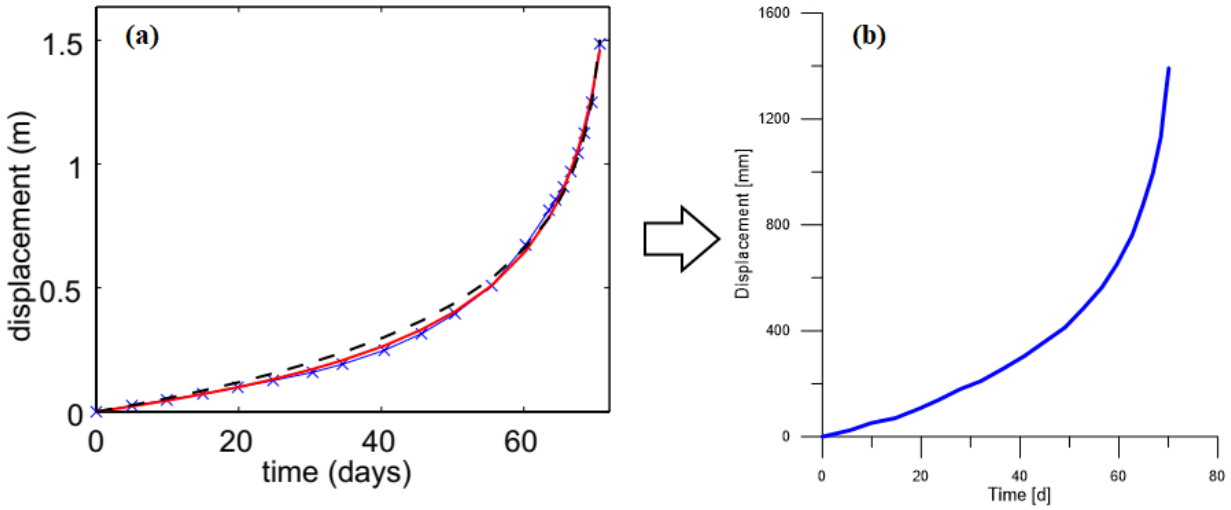


Fig. 1 - Example of a monitoring dataset digitizing operation. (a) Monitoring displacement vs time graph registered on benchmark #5 of the Vajont landslide (after Sornette et al., 2003), where displacements are reported in m; (b) Digitized dataset (in mm)

A time-of-failure forecast was performed following the Fukuzono method with the dataset obtained from this step. For each landslide, the predicted time of failure was computed by applying a linear regression corresponding to a value of $\alpha$=2 on the inverse-velocity versus time dataset.
As indicated and recommended by the scientific studies previously reported, the forecast model was applied to the accelerating phase to achieve higher accuracy in the time-of-failure prediction. The tertiary creep starting point, corresponding to the first datum of the inverse velocity model, was selected manually with the objective of minimizing the $R^2$ parameter, thus obtaining a more accurate fitting of the dataset available. Fig. 2 presents an example of this operation, referring to the Vajont benchmark #5 previously mentioned.

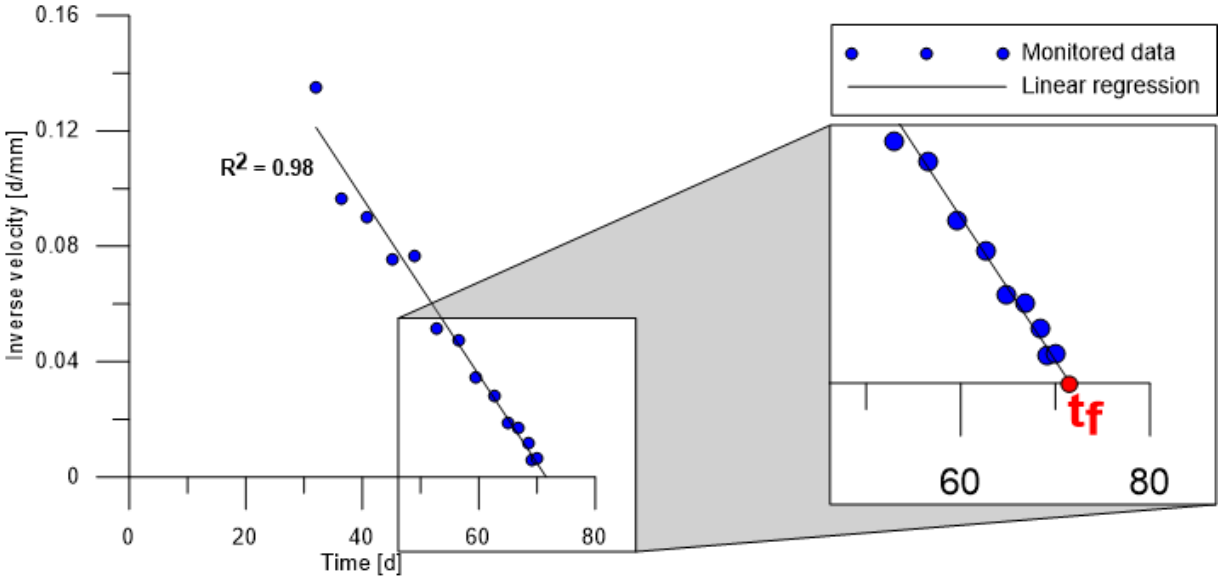


Fig. 2 - Example of the linear Fukuzono model application and the corresponding $R^2$ value, with a detail of the intersection between the linear regression and the x-axis

While the linear regression is considered a good approximation and has been used in different conditions as a valid failure forecasting method, taking into account the non-linear trend could allow a more accurate description of the landslide's behaviour before collapse is reached. For this reason, calibration of the *A* and $\alpha$ parameters was conducted for each single case after evaluating the time of failure, in order to better fit the monitored data. To achieve this goal, the GRG (Generalized Reduced Gradient) non-linear method implemented in the S*olver* add-in component of Microsoft Excel was used (a detailed review of this method can be found in Lasdon et al., 1974). The variation in parameters aims to minimize the Root Mean Square Error (RMSE).

### 2.4. Normalized velocity curves definition

Once the parameters of the Fukuzono model had been assessed, the possible behaviour of the landslide approaching failure could be described. In particular, the next step entailed the definition of a theoretical velocity versus time characteristic curve describing the landslide's predicted velocity at a certain temporal distance from collapse. This operation could be carried out under the assumption that the *A*, $\alpha$ and $t_f$ parameters provide a phenomenological description of the mechanical behaviour of the landslide approaching failure. Crosta and Agliardi (2002) used a similar methodology to define alert velocity thresholds for the Ruinon rockslide, with the main objective to deliver useful information regarding emergency management.

These curves resulted from the application of the following equation, derived from the Fukuzono-Voight model (Voight, 1988):

$$v_{FV} = \left(A(\alpha - 1)\left(t_f - t\right)\right)^{\frac{1}{1-\alpha}} \quad [3]$$

where $\alpha > 1$, $t_f > t$ and all the aforementioned parameters, relative to each single landslide, are taken into account. A time interval ranging from 0 to 30 days has been chosen in this paper, meaning that the curve represents the theoretical velocities reached by the landslide starting from 30 days before failure to the moment of collapse, identified by the presence of a vertical asymptote ($v_{FV} \to \infty$).

Each curve computed in this way must be considered site-specific, because the model parameters were inferred from the monitoring data of a particular case, and each landslide displayed unique displacement and velocity data. For these reasons, a comparison between velocity curves derived from different landslides is meaningless. To overcome this problem, the next step involved a procedure aimed to normalize the velocity data obtained by applying the model. The result of this operation was a new dimensionless velocity parameter $v_n$, which would allow a comparison between data acquired from different cases. In particular, the definition of a common trend in landslide evolution could prove very useful in the evaluation of generalized alert velocity thresholds.

To achieve this goal, the following formulation was proposed:

$$v_n = \frac{v_{FV} - \mu_{v_{FV}}}{\sigma_{v_{FV}}} \quad [4]$$

where $v_{FV}$ is the velocity previously obtained by applying Equation 3, while $\mu_{v_{FV}}$ and $\sigma_{v_{FV}}$ are the mean value and the standard deviation of the $v_{FV}$ values represented by the curve, respectively. The application of this procedure returned a normalized-velocity versus time curve, which can be used to define a generalized trend to describe the behaviour of a landslide approaching failure.

## 3. Results and discussion

### 3.1. Time-of-failure forecast

In this paper, the prediction of a landslide's time of failure was computed by applying the Fukuzono inverse velocity method, under the hypothesis of linear behaviour near collapse. This assumption was made since its combination of good predictions and simplicity of use has been highlighted in several scientific studies (Rose and Hungr, 2006; Gigli et al., 2011; Dick et al., 2015).

Results obtained from the back-analysis on the database of historical landslides, reported in Table 2, show that the linear regression of the datasets referring to the accelerating phase offers a good prediction of the time of failure. Out of the 26 cases included in this study, 11 were correctly forecasted by the inverse velocity method, obtaining a predicted time of failure equivalent to the actual day of collapse. Additionally, in 18 of the 26 cases examined the difference between effective and estimated time of failure $\Delta t_f$ is equal to or less than 3 days. Moreover, a large variability of the *A* parameter was noted, with a range of three orders of magnitude between extreme values.

Another parameter considered to assess the effectiveness of the model is the $R^2$ coefficient, which provides a measure of the accuracy of the linear regression applied to the datasets. This parameter ranges from 0 to 1, representing no correlation and perfect correlation respectively.

The results show that 62% of the cases present a value of $R^2$>0.9, while 81% are greater than 0.8 and 88% display a value of $R^2$>0.7. Small values of the correlation coefficient could be attributed to different factors, such as a landslide's behaviour diverging from linearity (i.e. asymptotic) or insufficient quality and/or quantity of monitoring data. In particular, evidence of inadequate monitoring data was noted throughout the digitizing operation. This aspect affects the accuracy of the model directly, as it performs better when high frequency monitoring data are available. Indeed, a detailed displacement representation could prove fundamental to accurately assess the future behaviour of the landslide.

| Name | Actual time of failure [d] | Forecasted time of failure [d] | $R^2$ [-] | Linear Regression | | Non-linear model | |
|---|---|---|---|---|---|---|---|
| | | | | A | α | A | α |
| **Afton Mine** | 69 | 69 | 0.95 | 0.0014 | 2.00 | 0.0016 | 1.94 |
| **Asamushi** | 7 | 7 | 0.85 | 0.0046 | 2.00 | 0.0056 | 1.96 |
| **Betze Post SE** | 45 | 45 | 0.99 | 0.0121 | 2.00 | 0.0119 | 2.00 |
| **Betze Post SW** | 5 | 5 | 0.99 | 0.0183 | 2.00 | 0.0173 | 2.01 |
| **Bomba** | 1320 | 1352 | 0.86 | 0.0041 | 2.00 | 0.0038 | 2.15 |
| **Braced up Cliff** | 1910 | 1904 | 0.92 | 0.0529 | 2.00 | 0.0548 | 1.53 |
| **Cavallerizzo** | 6 | 6 | 0.99 | 0.0654 | 2.00 | 0.0779 | 1.96 |
| **Chuquicamata** | 263 | 263 | 0.77 | 0.0006 | 2.00 | 0.0004 | 2.10 |
| **Delabole Quarry** | 5899 | 5954 | 0.74 | 0.0218 | 2.00 | 0.0205 | 1.96 |
| **Dosan Line** | 3 | 3 | 0.97 | 0.0105 | 2.00 | 0.0098 | 2.01 |
| **Hogart Pit** | 291 | 286 | 0.97 | 0.0022 | 2.00 | 0.0024 | 1.97 |
| **Huanglongxi** | 5 | 5 | 0.91 | 0.0151 | 2.00 | 0.0109 | 2.00 |
| **La Chenaula** | 884 | 890 | 0.29 | 0.0821 | 2.00 | 0.0767 | 1.94 |
| **La Saxe** | 21 | 21 | 0.95 | 0.0025 | 2.00 | 0.0135 | 1.77 |
| **Maoxian** | 1018 | 1020 | 0.94 | 0.0827 | 2.00 | 0.0777 | 1.93 |
| **Mt Beni** | 258 | 260 | 0.93 | 0.0002 | 2.00 | 0.0015 | 2.13 |
| **Nevis Bluff** | 287 | 279 | 0.98 | 0.0191 | 2.00 | 0.0191 | 2.00 |
| **Ohto** | 92 | 91 | 0.95 | 0.0303 | 2.00 | 0.0400 | 1.90 |
| **Ooigawa** | 9 | 9 | 0.99 | 0.1216 | 2.00 | 0.2813 | 1.85 |
| **Preonzo** | 13 | 13 | 0.64 | 0.0028 | 2.00 | 0.0024 | 2.03 |
| **Puigcercòs** | 2198 | 2264 | 0.88 | 0.0116 | 2.00 | 0.0106 | 1.94 |
| **Selborne** | 600 | 597 | 0.97 | 0.1495 | 2.00 | 0.1570 | 2.03 |
| **Town of Peace River** | 178 | 181 | 0.60 | 0.1241 | 2.00 | 0.1371 | 2.05 |
| **Tuckabianna West** | 38 | 37 | 0.88 | 0.0426 | 2.00 | 0.0343 | 2.07 |
| **Vajont** | 70 | 71 | 0.98 | 0.0307 | 2.00 | 0.0319 | 1.97 |
| **Xintan** | 2800 | 2805 | 0.88 | 0.0007 | 2.00 | 0.0008 | 2.00 |

Table 2 - Results obtained from the time of failure prediction and calibration procedures for each landslide included in the database

### 3.2. Model calibration

Calibration of *A* and *α* parameters was conducted to obtain a better representation of landslide behaviour in the final stage of its evolution towards failure (an example of this operation is reported in Fig. 3). This procedure could prove to be a significant factor since evaluation of the velocity-time curve depends on these parameters, thus a non-linear behaviour should be taken into consideration. Regarding parameter *α*, the results acquired from this operation and reported in Table 2 are consistent with the range of values obtained by Fukuzono (1985, 1989), being included within an interval of 1.5-2.2. While significant variations can be noted, it is worth reporting that for 14 out of 26 cases the absolute variation of *α* is less than 0.05 compared to the original $\alpha$=2 value. Furthermore, 19 out of 26 cases reported a variation of the *α* value to less than 0.1, while 24 out of 26 featured a $\Delta\alpha$<0.2. The calibration also showed that the majority of the landslides (13 versus 9) tends to assume a value of $\alpha$<2, corresponding to a convex trend in the inverse velocity plot. Regarding parameter *A*, the calibration showed an increment in the variation with the increasing of the divergence from the linear behaviour, reaching a difference of one order of magnitude in those cases where a pronounced non-linear trend is present.

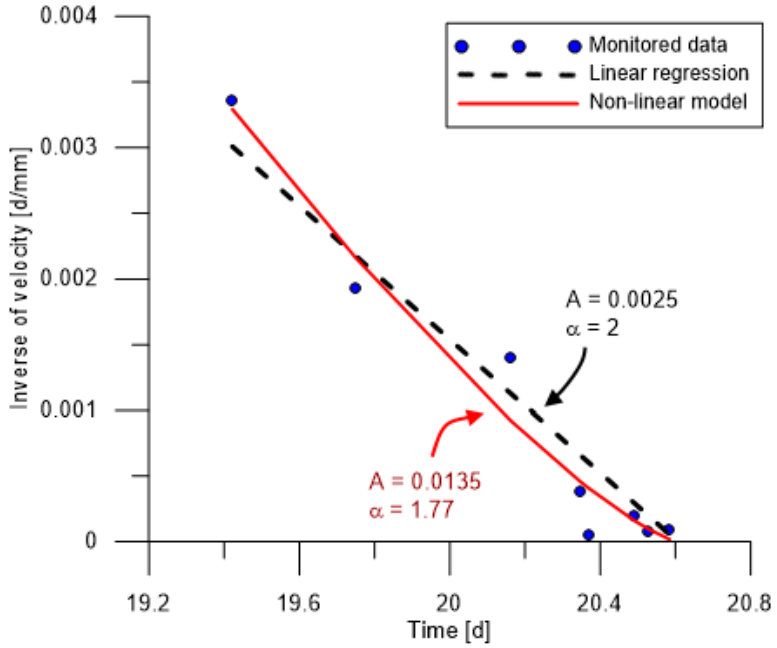


Fig. 3 - Comparison between the linear regression (black dashed line) and non-linear curve (red continuous line) obtained from the calibration procedure, with corresponding A and α parameters. The case presented refers to the La Saxe landslide, studied by Manconi and Giordan (2016)

### 3.3. Definition and normalization of velocity curves

The parameters obtained from the calibration and the forecasted time of failure $t_f$ were included in Equation 3 to define a characteristic velocity curve specifically for each case. The result is a curve, ranging from 0 to 30 days, describing the theoretical velocity value assumed by the landslide at a certain temporal distance from the collapse. As stated before, due to the variability and uniqueness of the parameters governing the model behaviour, the curves must be considered site-specific. For this reason, alert thresholds can be accurately assessed only when characteristic curves evaluated from local data are taken into account.

The theoretical velocities resulting from the model application were normalized by applying Equation 4 so as to overcome this problem. This procedure aims to define a new parameter that could allow the identification of a common trend between different cases. A time interval ranging from 0 to 30 was chosen to compare the curves, with a time step of 0.5 days, so as to frame all the cases included in the study in a single plot. The result of this operation, as showed in Fig. 4, is a graph containing a curve for each landslide monitored.

The dimensionless parameter obtained from the normalization increases its value with the approach of the collapse, located at $t$=0 days, where a vertical asymptote is reached. As can be seen from the resulting graph (Fig. 4), the normalization procedure successfully rescaled the velocity values. Nonetheless, a difference appears when the landslides approach failure, in particular at $t$=10 days from collapse the curves start to display a peculiar behaviour, which becomes more evident as the curves approach the vertical asymptote.

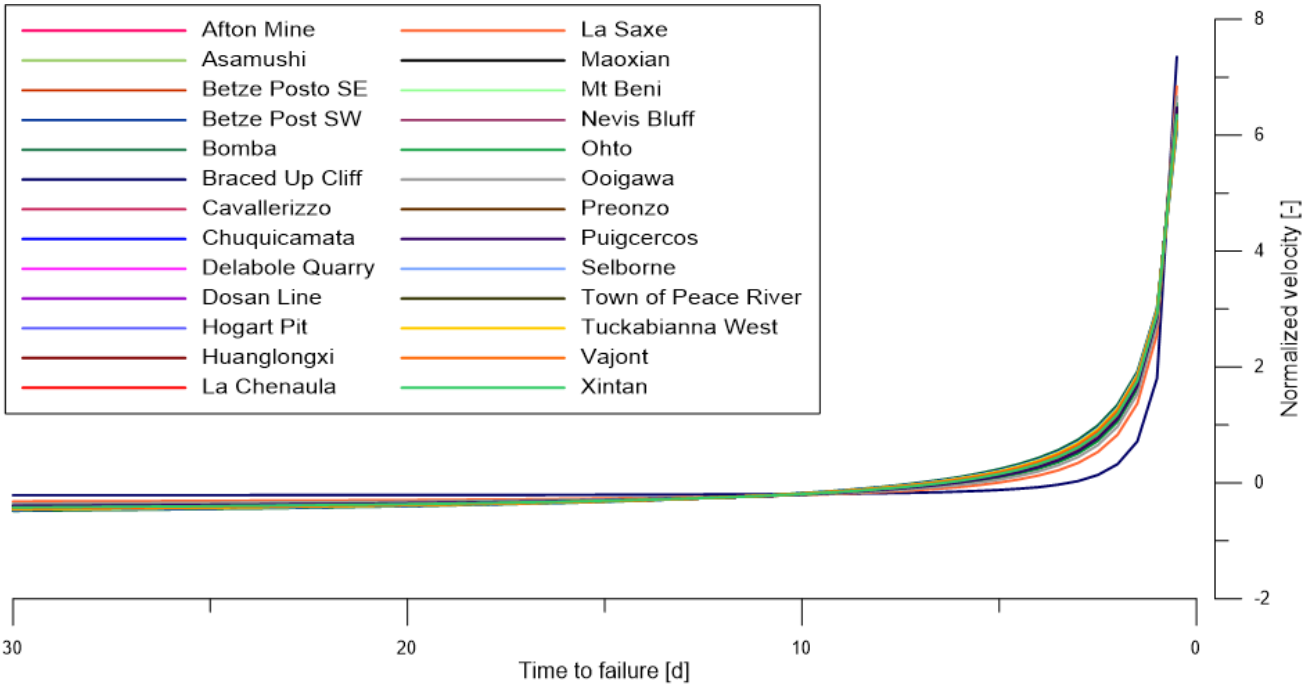


Fig. 4 – Normalized-velocity versus time plot, including all the cases considered in the present study

.

On analysis of the model, the dissimilarity seems to depend of the $\alpha$ parameter, which in the Fukuzono model represents the linearity or non-linearity of the trend. By taking the "linear" curve featuring $\alpha$=2 as reference, it can be noted that, when the non-linear behaviour is defined by a value of $\alpha$<2, the flex point where the curve changes its trend appears later. A value of $\alpha$>2 instead leads to an earlier increasing in terms of normalized velocity. The difference compared to the reference case becomes more evident as the behaviour diverges from linearity (i.e. Braced up Cliff in Fig. 4, featuring a value of $\alpha$=1.53). Additionally, one of the features emerging from the normalization of the velocity values is the negligibility of the *A* parameter, which plays no role in defining the dimensionless velocity curves. This could prove to be a very interesting aspect since this parameter can have a wide range of values, as shown in the present study, and a certain degree of uncertainty in the model is removed by neglecting this term. Following this line, each curve represented in a normalized-velocity versus time plot can be referred to the value of $\alpha$ derived from the calibration of the Fukuzono model, thus setting a generalized graph of reference to assess alert thresholds according to specific needs.

## 4. Application of the generalized criterion

In the process of developing the generalized criterion, the complete monitoring dataset was taken into account from the start of the accelerating phase to the last measure available before collapse for each landslide. This approach should not be considered as representative of a real case, where data are gradually acquired with the advancing of the monitoring activity. In order to test the procedure with a more realistic approach, in the following chapter another landslide, not included in the database, is presented and analysed by simulating progressive acquisition of monitoring data. Thanks to this approach, it should be possible to evaluate the efficiency of the criterion proposed and its ability to represent the behaviour of the landslide approaching failure.

The procedure will be applied according to the following steps:

a) Once the first point of the accelerating phase is identified, the following three data are taken into account to provide the starting dataset;
b) The inverse velocity method is applied to estimate the time-of-failure theoretical value, assuming the hypothesis of linearity in the $1/v - t$ trend;
c) Equation 3 is applied to compute the theoretical displacement velocities. The formulation includes linear *A* and $\alpha$ values;
d) The model calibration is carried out by minimizing the RMSE evaluated between the monitoring data and velocity data computed in the previous step;
e) The theoretical velocity curve is computed by using the value of $t_f$ evaluated in step b), and model parameters *A* and $\alpha$ obtained in step d);

f) By evaluating the mean and standard deviation of the velocity values computed in the previous step, the value obtained from the monitoring activity can be normalized according to Equation 4. This procedure should allow a comparison with the theoretical curve defined by a specific value of the $\alpha$ parameter;
g) When new monitoring data are available, they are added to the dataset and the procedure is repeated starting from step b).

### 4.1. The Kagemori Quarry landslide

The slope failure occurred on 20 September 1973 at Kagemori limestone quarry, located in the Saitama prefecture near Tokyo, Japan. Yamaguchi and Shimotani (1986) reported a rockslide slope movement with an estimated volume of 300'000-400'00 $m^3$ of limestone rock debris. According to the authors, the sliding surface observed after collapse was "irregular and complex", probably due to the influence of small-scale slides following the main failure. Fig. 5 reports the displacement dataset used to test the generalized criterion.

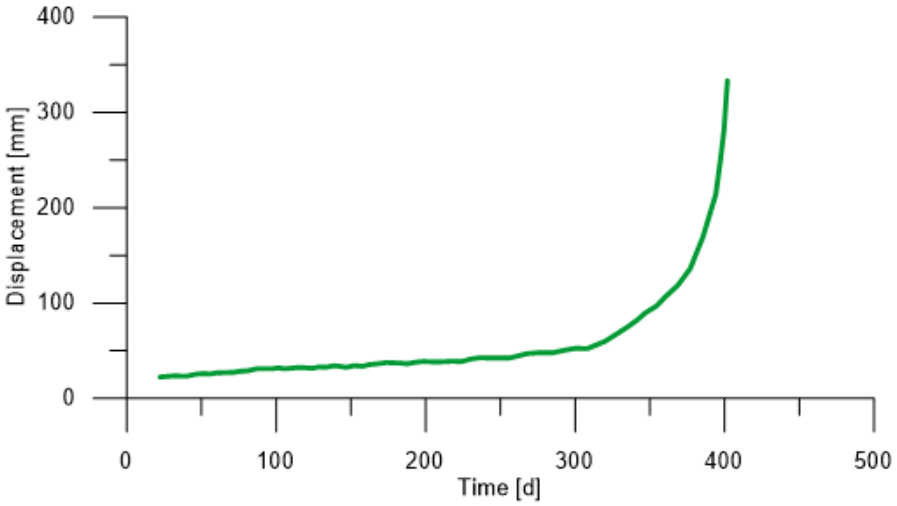


Fig. 5 - Displacement recorded at Kagemori Quarry before the collapse (data digitized from Yamaguchi and Shimotani, 1986)

As can be noted from the results of the time-of-failure prediction reported in Table 3, the inverse velocity method increases the forecast quality with the progressive addition of new monitoring data. Specifically, at $t$=397.2 days, the value of $t_f$ estimated by applying a linear regression coincides with the actual failure recorded at $t$=404 days. The two following iterations of the forecast procedure confirm the prediction, displaying the same $t_f$ value. According to these results, an accurate time-of-failure assessment could have been determined approximately 7 days before the actual collapse. Concerning the model calibration, it can be noted that parameters $A$ and $\alpha$ display relatively small variation throughout the evolution of the accelerating phase. In particular, 7 days before the slope failure, the calibration of the $\alpha$ coefficient returns a value of $\alpha$=2.05 which remains constant until the last monitoring data are received. The maximum variation observed for this parameter in previous steps is $\Delta\alpha$=0.01.

| Time $t$ [d] | Time of failure $t_f$ [d] | $\Delta t$ [d] | $A$ [-] | $\alpha$ [-] | $v_n$ [-] |
|---|---|---|---|---|---|
| 385.5 | 405.2 | 19.7 | 0.0137 | 2.06 | -0.3336 |
| 394.1 | 406.1 | 12.0 | 0.0141 | 2.04 | -0.2587 |
| 397.2 | 404.3 | 7.1 | 0.0146 | 2.05 | 0.1731 |
| 399.6 | 404.2 | 4.6 | 0.0148 | 2.05 | 0.3056 |
| 401.8 | 404.3 | 2.5 | 0.0148 | 2.05 | 0.8886 |

Table 3 - Results obtained from the time-of-failure forecast, model calibration and normalization procedures

The monitoring data available after the onset of acceleration (identified at $t$=360 days) are progressively added to the dataset and normalized by applying the procedure described at the beginning of this chapter. It is important to note that, for each instrumental measure, the values of $A$ and $\alpha$ could change from the ones estimated with the previous dataset. Therefore, it is fundamental to re-evaluate the velocity curve with the new calibrated parameters. This procedure should allow to obtain the updated values of $\mu_{v_{FV}}$ and $\sigma_{v_{FV}}$, to normalize the measured velocity properly.

The resulting non-dimensional coefficients $v_n$ can be compared with the theoretical generalized curve featuring the same value of the $\alpha$ parameter. According to the parameters resulting from the calibration phase, in this case the $\alpha$=2.05 curve

is taken into account. Fig. 6 displays a good correspondence between the monitoring data and the curve previously computed, highlighting the effectiveness of the generalized trend to represent the landslide's behaviour.

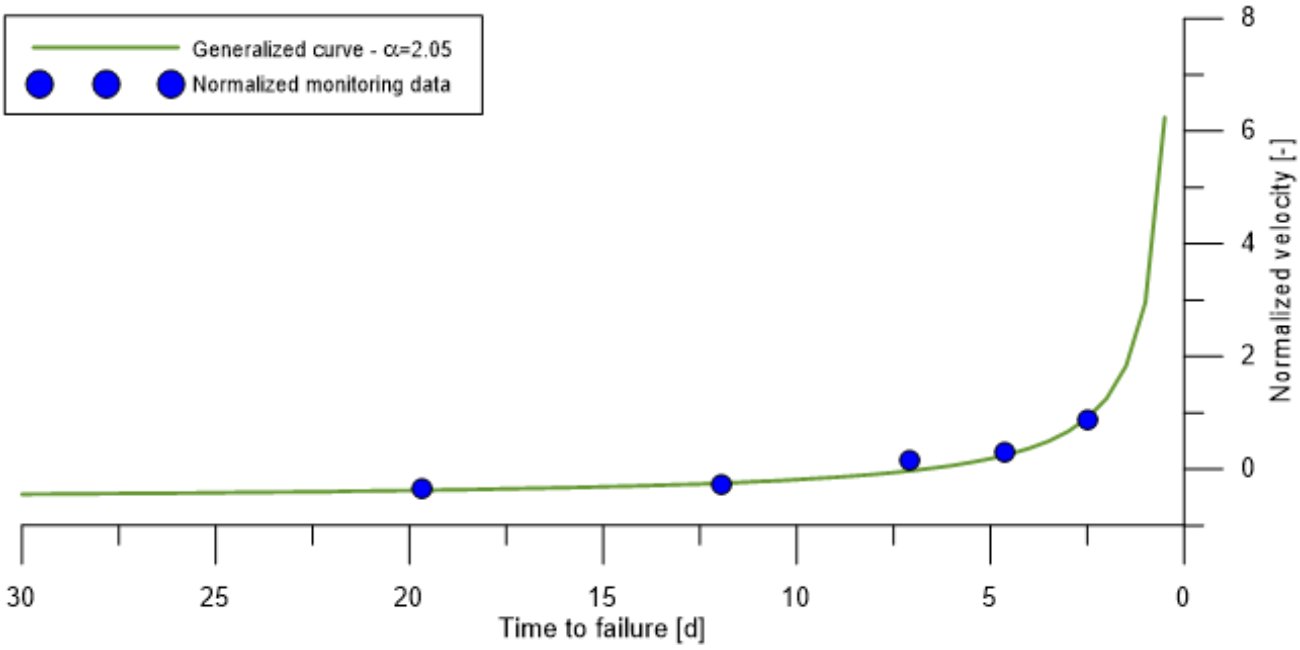


Fig. 6 - Comparison between normalized monitoring data and the generalized curve featuring the corresponding a value

## 5. Conclusions and final remarks

In this study, a procedure to describe a generalized criterion useful to compare events with different features and to help define alert thresholds has been established. To achieve this goal, a database of historical landslides was created in order to perform a back-analysis on the datasets available. For each single case, the time of failure was computed through the application of the inverse velocity method developed by Fukuzono (1985). The results obtained from this step showed high accuracy of the model under the hypothesis of linearity when applied on the final stage of the landslide evolution, defined by an accelerating trend and described by the tertiary phase of the creep theory. Furthermore, to better adapt the model to the monitored data, calibration of the two empirical parameters $A$ and $\alpha$ was carried out. For the events reported in this study, the values of $\alpha$ are compatible with the standard range relative to natural slopes (1.5 to 2.2); furthermore, the calibrated value of many of the cases is quite close to the linearity reference. With the newly computed parameters, a theoretical curve has been derived for each case, describing the displacement velocity predicted at a certain time before collapse. In order to generalize these curves and compare landslides displaying different features, a normalization procedure was conducted, thus obtaining a new dimensionless parameter. Due to the correspondence between these new values, this operation allowed overcoming the site-specific feature and representing all the landslides included in the database in a single chart. Notably, these curves have no dependence on parameter A, while the variation of parameter α influences their behaviour when approaching collapse. Finally, the criterion was applied to a different case by simulating progressive data acquisition. This analysis evidenced that the method proposed can provide an effective tool to describe the theoretical behaviour of the landslide during the accelerating phase. The results obtained for this specific case indicate that, by analysing the displacement data, the correct time of failure of the Kagemori Quarry landslide could have been predicted about 7 days before the actual collapse.

While the procedure presented successfully achieved the initial purpose of this paper, it is worth reporting some final considerations about the method described in this study.

All the displacements data reported in scientific literature and employed in this study refer to the slope surface, with no information available concerning underground behaviour. This could prove to be an important factor when complex landslides are taken into account, since surface and underground behaviour can be significantly different. Following this approach, Ishizawa et al. (2013) presented a study regarding the effectiveness of underground displacement monitoring on a sand model slope.

As stated above, the inverse velocity method must be applied on the accelerating phase of the landslide. However, a universal method to identify the exact point where the transition between secondary and tertiary creep takes place has not been developed yet.

## 6. References


Atzeni, C., Barla, M., Pieraccini, M., Antolini, F., 2015. Early warning monitoring of natural and engineered slopes with Ground-Based Synthetic-Aperture Radar. Rock Mechanics and Rock Engineering (2015) 48:235-246. DOI: https://doi.org/10.1007/s00603-014-0554-4

Boyd, JM., Hinds, DV., Moy, D., Rogers, C., 1973. Two simple devices for monitoring movements in rock slopes. Quarterly Journal of Engineering Geology and Hydrogeology (1973), 6(3-4):295-302. DOI: https://doi.org/10.1144/GSL.QJEG.1973.006.03.12

Bozzano, F., Cipriani, I., Mazzanti, P., Prestininzi, A., 2014. A field experiment for calibrating landslide time-of-failure prediction functions. International Journal of Rock Mechanics & Mining Sciences 67 (2014) 69-77. DOI: https://doi.org/10.1016/j.ijrmms.2013.12.006

Brawner, CO., Stacey, PF., 1979. Hogart Pit slope failure, Ontario, Canada. In Rockslides and Avalanches, B; Elsevier: Amsterdam, The Netherlands, 1979: pp. 691-70. DOI: https://doi.org/10.1016/B978-0-444-41508-0.50029-6

Brown, I., Hittinger, M., Goodman, R., 1980. Finite element study of the Nevis Bluff (New Zealand) rock slope failure. Rock Mechanics, 12, 231-245 (1980). DOI: https://doi.org/10.1007/BF01251027

Carlà, T., Farina, P., Intrieri, E., Botsialas, K., Casagli, N., 2017a. On the monitoring and early-warning of brittle slope failures in hard rock masses: Examples from an open-pit mine. Engineering Geology 228 (2017) 71-81. DOI: https://doi.org/10.1016/j.enggeo.2017.08.007

Carlà, T., Intrieri, E., Di Traglia, F., Nolesini, T., Gigli, G., Casagli, N., 2017b. Guidelines on the use of inverse velocity method as a tool for setting alarm thresholds and forecasting landslides and structure collapses. Landslides (2017) 14:517-534. DOI: https://doi.org/10.1007/s10346-016-0731-5

Carlà, T., Macciotta, R., Hendry, M., Martin, D., Edwards, T., Evans, T., Farina, P., Intrieri, E., Casagli, N., 2018. Displacement of a landslide retaining wall and application of an enhanced failure forecasting approach. Landslides (2018) 15:489-505. DOI: https://doi.org/10.1007/s10346-017-0887-7

Cornelius, R., Voight, B., 1995. Graphical and PC-software analysis of volcano eruption precursors according to the Material Failure Forecast Method (FFM). Journal of Volcanology and Geothermal Research, 64 (1995) 295-320. DOI: https://doi.org/10.1016/0377-0273(94)00078-U

Crosta, GB., Agliardi, F., 2002. How to obtain alert velocity thresholds for large rockslides. Physics and Chemistry of the Earth 27 (2002) 1557-1565. DOI: https://doi.org/10.1016/S1474-7065(02)00177-8

Crosta, GB., Agliardi, F., 2003. Failure forecast for large rock slides by surface displacement measurements. Canadian Geotechnical Journal 40: 176-191 (2003). DOI: https://doi.org/10.1139/t02-085

Cruden, DM., Masoumzadeh, S., 1987 Accelerating creep of the slopes of a coal mine. Rock Mechanics and Rock Engineering 20,123-13. DOI: https://doi.org/10.1007/BF01410043

Dick, GJ., Eberhardt, E., Gabrejo-Liévano, AG., Stead, D., Rose, ND., 2015. Development of an early-warning time-of-failure analysis methodology for open-pit mine slopes utilizing ground-based slope stability radar monitoring data. Canadian Geotechnical Journal 52:515-529 (2015). DOI: https://doi.org/10.1139/cgj-2014-0028

Federico, A., Popescu, M., Elia, G., Fidelibus, C., Internò, G., Murianni, A., 2012. Prediction of time to slope failure: a general framework. Environmental Earth Sciences (2012) 66:245-256. DOI: https://doi.org/10.1007/s12665-011-1231-5

Fukuzono, T., 1985. A new method for predicting the failure time of a slope. In Proceedings of the Fourth International Conference and Field Workshop on Landslides (Tokyo; 1985). Tokyo University Press. 1985:145–150

Fukuzono, T., 1989. A simple method for predicting the failure time of a slope using reciprocal of velocity. Technology for Disaster Prevention, Science and Technology Agency, Japan. International Coop Agency, Japan 1(13):111–128

Fukuzono, T., 1990. Recent studies on time prediction of slope failure. Landslide News 4:9-12

Geoprævent, 2012. Rockfall monitoring Preonzo: Detailed monitoring and analysis of rock movements by interferometric radar (GB-InSAR). Available online at: www.geopraevent.ch (Last access on January 29th, 2018)

Gigli, G., Fanti, R., Canuti, P., Casagli, N., 2011. Integration of advanced monitoring and numerical modelling techniques for the complete risk scenario analysis of rockslides: The case of Mt. Beni (Florence, Italy). Engineering Geology 120 (2011) 48-59. DOI: https://doi.org/10.1016/j.enggeo.2011.03.017

Glastonbury, J., Fell, R., 2002. Report on the analysis of the deformation behaviour of excavated rock slopes. School of Civil and Environmental Engineering, University of New South Wales, Report n° R403

Herrera, G., Gutiérrez, F., Garcìa-Davalillo, JC., Guerrero, J., Notti, D., Galve, JP., Fernàndez-Merodo, JA., Cooksley, G., 2013. Multi-sensor advanced DInSAR monitoring of very slow landslides: The Tena Valley case study (Central Spanish Pyrenees). Remote Sensing of Environment, Volume 128, 21 January 2013, pages 31-43. DOI: https://doi.org/10.1016/j.rse.2012.09.020

Intrieri, E., Gigli, G., 2016. Landslide forecasting and factors influencing predictability. Natural Hazards and Earth System Sciences, 16, 2501-2510, 2016. DOI: https://doi.org/10.5194/nhess-16-2501-2016

Intrieri, E., Gigli, G., Mugnai, F., Fanti, R., Casagli, N., 2012. Design and implementation of a landslide early warning system. Engineering Geology 147-148 (2012) 124-136. DOI: https://doi.org/10.1016/j.enggeo.2012.07.017

Intrieri, E., Raspini, F., Fumagalli, A., Lu, P., Del Conte, S., Farina, P., Allievi, J., Ferretti, A., Casagli, N., 2018. The Maoxian Landslide as seen from space: detecting precursor of failure with Sentinel-1 data. Landslides, January 2018, Vol.15, Issue 1, pp 123-133. DOI: https://doi.org/10.1007/s10346-017-0915-7

Iovine, G., Petrucci, O., Rizzo, V., Tansi, C., 2006. The March 7th Cavallerizzo (Cerzeto) Landslide in Calabria – Southern Italy. IAEG Congress, Nottingham, UK 2006 Paper number 785

Ishizawa, T., Sakai, N., Morohoshi, T., Fukuzono, T., 2013. Effectiveness of underground displacement measurement using inclinometer for prediction of slope failure. Landslides – Journal of the Japan Landslide Society Vol.50, n°6 (2013), November, pp.256-267 (in Japanese). DOI: https://doi.org/10.3313/jls.50.256

Keqiang, H., Sijing, W., 2006. Double parameter threshold and its formation mechanism of the colluvial landslide: Xintan landslide, China. Environmental Geology 2006, 49, 696-707. DOI: https://doi.org/10.1007/s00254-005-0108-x

Kilburn, CRJ., Petley, DN., 2003. Forecasting giant, catastrophic slope collapse: lessons from Vajont, Northern Italy. Geomorphology 54 (2003) 21-32. DOI: https://doi.org/10.1016/S0169-555X(03)00052-7

Kim, TH., Cruden, DM., Martin, D., Froese, CR., Morgan, AJ., 2010. Landslide movements and their characteristic, Town of Peace River, Alberta. Conference Paper, from 63rd Canadian Geotechnical Conference and 6th Canadian Permafrost Conference, at Calgary, Alberta

Lasdon, LS., Fox, RL., Ratner, MW., 1974. Nonlinear optimization using the generalized reduced gradient method. RAIRO-Operations Research – Recherche Opérationelle Vol.8 Issue 3, pp. 73-103

Li, X., Jiming, K., Zhenyu, W., 2012. Landslide displacement prediction based on combining method with optimal weight. Natural Hazards (2012) 61: 635-646. DOI: https://doi.org/10.1007/s11069-011-0051-y

Manconi, A., Giordan, D., 2015. Landslide early warning based on failure forecast models: the example of the Mt. de la Saxe rockslide, northern Italy. Natural Hazards and Earth System Sciences, 15, 1639-1644, 2015. DOI: https://doi.org/10.5194/nhess-15-1639-2015

Manconi, A., Giordan, D., 2016. Landslide failure forecast in near-real time. Geomatics, Natural Hazards and Risk, 2016, Vol.7, n°2, 639-648. DOI: https://doi.org/10.1080/19475705.2014.942388

Mazzanti, P., Bozzano, F., Cipriani, I., Prestininzi, A., 2017. New insights into the temporal prediction of landslides by a terrestrial SAR interferometry monitoring case study. Landslides (2015) 12:55-68. DOI: https://doi.org/10.1007/s10346-014-0469-x

Moretto, S., Bozzano, F., Esposito, C., Mazzanti, P., Rocca, A., 2017. Assessment of landslide pre-failure monitoring and forecasting using satellite SAR interferometry. Geosciences 2017, 7, 36. DOI: https://doi.org/10.3390/geosciences7020036

Mufundirwa, A., Fujii, Y., Kodama, J., 2010. A new practical method for prediction of geomechanical failure-time. International Journal of Rock Mechanics & Mining Sciences 47 (2010) 1079–1090. DOI: https://doi.org/10.1016/j.ijrmms.2010.07.001

Noverraz, F., Bonnard, C., 1992. Le glissement rapide de La Chenaula. Internationales Symposium INTERPRAEVENT 1992 – Bern, pp. 65-76 (in French)

Petley, DN., 2004. The evolution of slope failures: mechanisms of rupture propagation. Natural Hazards and Earth System Science, Copernicus Publications on behalf of the European Geosciences Union, 2004, 4 (1), pp.147-152

Rose, ND., Hungr, O., 2006. Forecasting potential rock slope failure in open pit mines – contingency planning and remediation. International journal of Rock Mechanics and Mining Science, February 17, 2006

Rose, ND., Hungr, O., 2007. Forecasting potential rock slope failure in open pit mines using the inverse-velocity method. International Journal of Rock Mechanics and Mining Science 2007; 44:308–32. DOI: https://doi.org/10.1016/j.ijrmms.2006.07.014

Royán, MJ., Abellán, A., Vilaplana, JM., 2015. Progressive failure leading to the 3 December 2013 rockfall at Puigcercós scarp (Catalonia, Spain). Landslides (2015) 12:585-595. DOI: https://doi.org/10.1007/s10346-015-0573-6

Saito, M., 1969. Forecasting time of slope failure by tertiary creep. In Proceedings of the Seventh International Conference on Soil Mechanics Foundation Engineering, 1969; 2:677–683

Saito, M., 1979. Evidential study on forecasting occurrence of slope failure. Trans. of the Dept. of Geomech. - Armenian Academy of Sciences, Yerevan, URSS

Saito, M., Uezawa, H., 1961. Failure of soil due to creep. In Fifth International Conference on Soil Mechanics and Foundation Engineering, 1: 315-318, Paris

Sättele, M., Kautblatter, M., Bründl, M., Straub, D., 2016. Forecasting rock slope failure: how reliable and effective are warning systems? Landslides (2016) 13:737. DOI: https://doi.org/10.1007/s10346-015-0605-2

Schumm, SA., Chorley, RJ., 1964. The fall of Threatening Rock. American Journal of Science, Vol. 262, November 1964, 1041-1054. DOI: https://doi.org/10.2475/ajs.262.9.1041

Sornette, D., Helmstetter, A., Andersen, JV., Gluzman, S., Grasso, JR., Pisarenko, V., 2004. Towards landslide predictions: two case studies. Physica A 338 (2004) 605-632. DOI: https://doi.org/10.1016/j.physa.2004.02.065

Suwa, H., Mizuno, T., Ishii, T., 2010. Prediction of a landslide and analysis monitoring of slide motion with reference to the 004 Ohto slide in Nara, Japan. Geomorphology 124 (2010) 157-163

Tavenas, F., Leroueil, S., 1981. Creep and failure of slopes in clays. Canadian Geotechnical Journal, 18 (1):106-120. DOI: https://doi.org/10.1139/t81-010

Ter-Stepanian, G., 1980. Creep on natural slopes and cutting. In Proceedings of the third International Symposium on Landslides, 2:95-108, New Delhi

Terzaghi, K., 1950. Mechanism of landslides. In Application of Geology to Engineering Practice (Berkeley Volume); Geological Society of America: Washington, DC, USA, 1950; pp. 83–123

Urciuoli, G., Picarelli, L., 2008. Interaction between landslides and man-made works. Landslides and Engineered Slopes – Chen et al. (eds) 2008, Taylor & Francis Group, London

Voight, B., 1988. A method for prediction of volcanic eruptions. Nature 1988; 332:125-130. DOI: https://doi.org/10.1038/332125a0

Voight, B., 1989. A relation to describe rate-dependent material failure. Science 1989; 243:200–203. DOI: https://doi.org/10.1126/science.243.4888.200

Voight, B., 1990. The 1985 Nevado del Ruiz volcano catastrophe: anatomy and retrospection. Journal of Volcanology and Geothermal Research, 44 (1990) 349-386. DOI: https://doi.org/10.1016/0377-0273(90)90027-D

Voight, B., Kennedy, BA., 1979. Slope failure of 1967-1969, Chuquicamata mine, Chile. In Developments of Geotechnical Engineering, Volume 14, part B, 1979, Pages 595-632. DOI: https://doi.org/10.1016/B978-0-444-41508-0.50025-9

Wasowski, J., Bovenga, F., 2014. Investigating landslides and unstable slopes with satellite Multi Temporal Interferometry: Current issues and future perspectives. Engineering Geology 174 (2014) 103-138. DOI: https://doi.org/10.1016/j.enggeo.2014.03.003

Wasowski, J., Bovenga, F., Dijkstra, T., Xingmin, M., Nutricato, R., Chiaradia, MT., 2014. Interferometry provides insight on slope deformations and landslides activity in the mountains of Zhouqu, Gansu, China. In Sassa K, Canuti P, Yin Y. (eds) Landslide Science for a Safer Geoenvironment. Springer, Cham. DOI: https://doi.org/10.1007/978-3-319-05050-8_56

Yamaguchi, U., Shimotani, T., 1986. A case study of slope failure in a limestone quarry. International Journal of Rock Mechanics and Mining Sciences & Geomechanics Abstracts, Volume 23, Issue 1, February 1986, Pages 95-104. DOI: https://doi.org/10.1016/0148-9062(86)91670-0

***FIGURES DIMENSION AND COLOUR***

| Fig. | Column-fitting width | Colour |
|---|---|---|
| 1 | 2 | Yes |
| 2 | 2 | Yes |
| 3 | 1.5 | Yes |
| 4 | 2 | Yes |
| 5 | 1.5 | Yes |
| 6 | 2 | Yes |